Optimized Rigid Motion Correction from Multiple Non-simultaneous X-Ray Angiographic Projections

Abhirup Banerjee[1,2,3(✉)] , Robin P. Choudhury[1,2], and Vicente Grau[3]

[1] Oxford Acute Vascular Imaging Centre, Oxford, UK
[2] Radcliffe Department of Medicine, Division of Cardiovascular Medicine,
University of Oxford, Oxford, UK
{abhirup.banerjee,robin.choudhury}@cardiov.ox.ac.uk
[3] Department of Engineering Science,
Institute of Biomedical Engineering, University of Oxford, Oxford, UK
vicente.grau@eng.ox.ac.uk

Abstract. X-ray angiography is the most commonly used medical imaging modality for the high resolution visualization of lumen structure in coronary arteries. Since the interpretation of 3D vascular geometry using multiple 2D image projections results in high intra- and inter-observer variability, the reconstruction of 3D coronary arterial (CA) tree is necessary. The automated 3D CA tree reconstruction from multiple 2D projections is challenging due to the existence of several imaging artifacts, most importantly the respiratory and cardiac motion. In this regard, the aim of the proposed work is to remove the effects of motion artifacts from non-simultaneous angiographic projections by developing a new iterative method for rigid motion correction. Our proposed approach is based on the optimal estimation of rigid transformation, occurred due to motion in the 3D tree, from each projection. The performance of the technique is qualitatively and quantitatively demonstrated using multiple angiographic projections of the left anterior descending, left circumflex, and right coronary artery from 15 patients.

Keywords: Motion correction · Rigid motion · 3D coronary tree reconstruction · X-ray angiograms

1 Introduction

Invasive coronary angiography (ICA) is the most commonly used imaging modality for the detection of coronary stenoses. Its advantages include simplicity, high spatial and temporal resolution of lumen structure, and most importantly, its utility to guide coronary interventions in real time [11]. However, despite these

clinical advantages, x-ray angiograms pose several challenges, especially in relation to visualizing lesion adequately and judging lesion severity. The 2D projections of 3D vascular structure in different image planes contain significant motion artifacts, including cardiac, respiratory, and patient or device movement, which makes the interpretation of 3D geometry difficult for the cardiologists. This leads to high intra- and inter-observer variability in understanding the anatomical structure and, in turn, affects the lesion severity assessment [6]. In addition, potential adverse effects of higher amount of radiographic contrast agent and exposure to x-rays limit the number of image acquisitions. To overcome these inherent limitations of ICA, 3D reconstruction of CA trees from multiple 2D x-ray projections has been attempted by a number of research groups [1–3,7].

Several of these 3D CA tree reconstruction methods can deal with problems such as vessel overlap, foreshortening, suboptimal projection angles, and tortuosity and eccentricity [3,4]. In order to obtain the acquisition geometry, some reconstruction methods rely on a prior calibration step [13], while others prefer non-calibrated data for reducing table movements during image acquisition and noise in calibrated parameters [2,5]. In cardiac interventions, single-plane systems are usually preferred over biplane systems due to the lower cost and the possibility of generating multiple x-ray angiograms. However, single-plane systems generate non-simultaneous projections, which are prone to several motion artifacts, including mainly patient or imaging device related movements, respiratory motion, and cardiac motion. Although the patient or imaging device related movements can be minimized by following a careful protocol during image acquisition [2], this is difficult to achieve for respiratory motion and not possible for heart beating motion. Even if short acquisitions can be captured during breath-hold, potential misregistration artifacts still remain, affecting geometry conditions [8]. Additionally, the patients are often not able to follow the breath-hold protocol. To overcome the motion artifacts due to cardiac movements, retrospective gating is commonly utilized, where image frames are selected from the same cardiac phase. This is usually achieved using the ECG signal acquired simultaneously with the angiograms. In most of the existing reconstruction methods, the frames are selected from the end of the diastolic phase when heart motion is minimal, such that no cardiac motion can be assumed between projections [10,12]. However, this assumption does not hold in a single-plane x-ray system.

In this regard, the purpose of our work is to generate a retrospective method for rigid motion correction from multiple x-ray projections. The optimal rigid transformation is iteratively estimated for each angiographic acquisition, to adjust for the relative rigid motion, generated from respiration and patient or device movements. The proposed method is formulated using a theorem regarding the geometry of a 3D object. The performance of the proposed motion correction technique is qualitatively and quantitatively evaluated over angiographic projections of both left coronary artery (LCA) and right coronary artery (RCA) from 15 patients, admitted in the hospital for suspected coronary stenosis. The algorithm results in average reprojection error of 0.504 mm after rigid motion correction, from left anterior descending (LAD), left circumflex (LCx) and RCA.

2   Proposed Rigid Motion Correction

2.1   Proposed Theorem

Theorem 1. *After rigid transformation of a 3D object, the 2D projection will remain equal if the source and projection plane are modified using the same rigid transformation.*

Proof. Let us assume the 3D object be A. The location of the x-ray source be S, any point on the projection plane be M, and the normal to the projection plane be N. So, any line passing through S and A is given by

$$Q = S + \alpha(A - S). \tag{1}$$

Since Q lies on the projection plane with a point M and the normal N, $\alpha = \frac{(M-S)\cdot N}{(A-S)\cdot N}$. Now, A is generated after rigid transformation (R, t), rotation R and translation t, on 3D object A^*. So, $A = RA^* + t$. Hence, (1) is rewritten as

$$Q = R(S^* + \alpha(A^* - S^*)) + t, \quad \text{where } S^* = R^{-1}(S - t)$$

Additionally, $\alpha = \frac{(M^*-S^*)\cdot N^*}{(A^*-S^*)\cdot N^*} = \alpha^*$, where $M^* = R^{-1}(M - t)$ and $N^* = R^T N$. So, $Q = R\,Q^* + t$, where $Q^* = S^* + \alpha^*(A^* - S^*)$. Hence, Q^* is a 3D object passing though 3D object A^* and source S^*. Now, we just need to show: Q^* lies on a 2D plane with a point M^* and normal N^*.

$$(Q^* - M^*) \cdot N^* = (R^{-1}(S - M + \alpha(A - S)))^T (R^T N) = (Q - M) \cdot N = 0$$

Hence, if Q is the projection of 3D object A from source S to a plane with point M and normal N, then, for any rigid transformation (R, t), $R^{-1}(Q - t)$ is the projection of $R^{-1}(A - t)$ from source $R^{-1}(S - t)$ on plane with point $R^{-1}(M - t)$ and normal $R^T N$. Since 3D rigid transformation of a 2D plane in 3D does not change the geometry, $R^{-1}(Q - t)$ continues to be the same 2D projection. Additionally, (R, t) transforms any plane with point M and normal N to the plane with point $R^{-1}(M - t)$ and normal $R^T N$. Hence, it suffices to say that, after rigid transformation, 2D projection of a 3D object remain equal if the source and projection plane are modified using the same rigid transformation.

2.2   Rigid Motion Estimation in Object-Domain

One major issue in 3D CA tree reconstruction is the latent motion in acquired angiograms from different views. Even after choosing end-diastole frames for non-simultaneous acquisition, the selected frame from a discrete set retains some temporal misalignment, leading to deformations in coronary vessels. Respirations cause, mostly rigid, transformation in heart and hence, in vessels. Movements in patient or device during acquisitions result in similar rigid motion.

In order to remove the rigid motion artifacts, the proposed approach estimates the optimal transformations from all angiographic acquisitions, minimizing the orthogonal distance between corresponding landmarks in object domain.
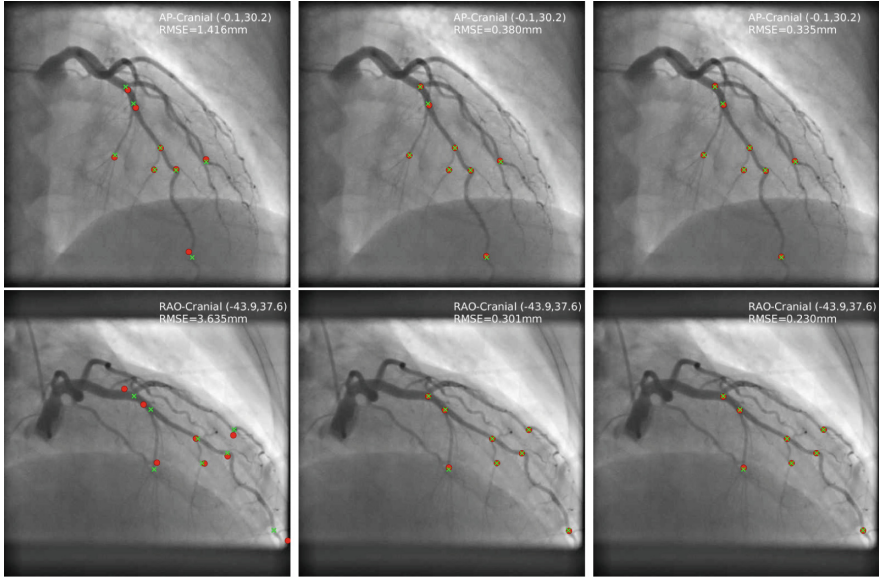
Fig. 1. Removing rigid motion from two projections (red: motion corrected landmarks, green: original landmarks). Left to right: initialization, iteration 5, and at convergence. (Color figure online)

Our proposed rigid motion correction method involves the identification of few (preferably 4–6) corresponding landmarks from all projections. In our method, the vessel bifurcations are manually identified for this purpose. Although, in 3D space, 3 landmarks are theoretically sufficient for estimating a rigid transformation, we prefer to use at least 4, due to high amount of motion artifacts.

Let us assume r rigid motion corrected 3D landmarks as $B_i; i = 1, \cdots, r$ and the projected landmark B_i on jth image plane as b_{ij} for $j = 1, \cdots, s$. Let us also assume the locations of x-ray source, a representative point on projection plane j, and the normal to the plane are defined as F_j, M_j, and N_j, respectively. Since B_i's are unknown, they are initially estimated as the nearest point of intersection of 3D projection lines $\overrightarrow{F_j b_{ij}}, j = 1, \cdots, s$,

$$B_i = \arg\min_p \sum_{j=1}^{s} D(p, \overrightarrow{F_j b_{ij}}), \qquad (2)$$

where $D(p, \overrightarrow{F_j b_{ij}})$ denotes the orthogonal distance from any point p to $\overrightarrow{F_j b_{ij}}$. Let us also define $B_{i,j}$ as the nearest point on $\overrightarrow{F_j b_{ij}}$ from B_i. Note that, $B_{i,j}$ is the location of the rigid motion affected 3D landmark B_i during jth image acquisition. Our aim is to measure the optimal rigid transformation (translation t_j and rotation R_j) for each acquisition $j = 1, \cdots, s$, so that the 3D landmarks

$B_{i,j}, i = 1, \cdots, r$ match with the corresponding 3D landmarks B_i, i.e.

$$\arg\min_{t_j, R_j} \sum_{i=1}^{r} \|B_i - (t_j + R_j B_{i,j})\| \quad \forall j = 1, \cdots, s. \tag{3}$$

Algorithm 1. Proposed Rigid Motion Correction

    Input   : Image frames at end-diastole from each projection plane
    Output: Rigid motion corrected image frames
1 Select n vessel landmarks (preferably $4-6$) from all projection planes;
2 do
3 | Estimate the rigid motion corrected 3D landmarks as the nearest orthogonal
      | point of 3D projection lines connecting vessel landmarks on projection
      | planes with the source (using (2) and (4));
4 | Estimate the optimal rigid transformation for each acquisition so that the
      | 3D landmarks match with rigid motion corrected landmarks (using (3));
5 while *the 3D landmarks for each image acquisition do not coincide*;
6 Return the optimal transformation that minimizes the effect of rigid motion.

The optimal transformation in Eq. (3) is estimated by Horn's quaternion-based method [9]. As the original 3D rigid motion corrected landmarks are not known, an iterative algorithm is developed, where, in every iteration, the 3D landmarks are measured using Eq. (2) and then the optimal rigid transformations are estimated using Eq. (3). In each iteration, the sources and landmarks on projection planes are updated based on the rigid transformation

$$F_{j'} = t_j + R_j F_j \quad \text{and} \quad b_{ij'} = t_j + R_j b_{ij}, \tag{4}$$

as per the theorem developed in previous subsection. An example of the result of the iterative minimization of rigid motion artifact from two projections (AP-cranial and RAO-cranial) of the LCA is depicted in Fig. 1. The pseudo-code of the proposed approach is presented in Algorithm 1.

3   Experimental Results

The performance of the proposed rigid motion correction algorithm is qualitatively as well as quantitatively demonstrated on 15 patients enrolled in clinical studies. For each patient, 2–3 angiographic projections are captured for RCA, while 3–6 angiographic projections are generated for LCA. Since the LAD and LCx arteries are generally not optimally visible at the same angiographic projection, different sets of LCA images are used for LAD and LCx arteries. The LAD, LCx, and RCA arteries are visible from at least two projections in 14, 13, and 12 patients, respectively, out of the total 15 patients. The proposed rigid motion
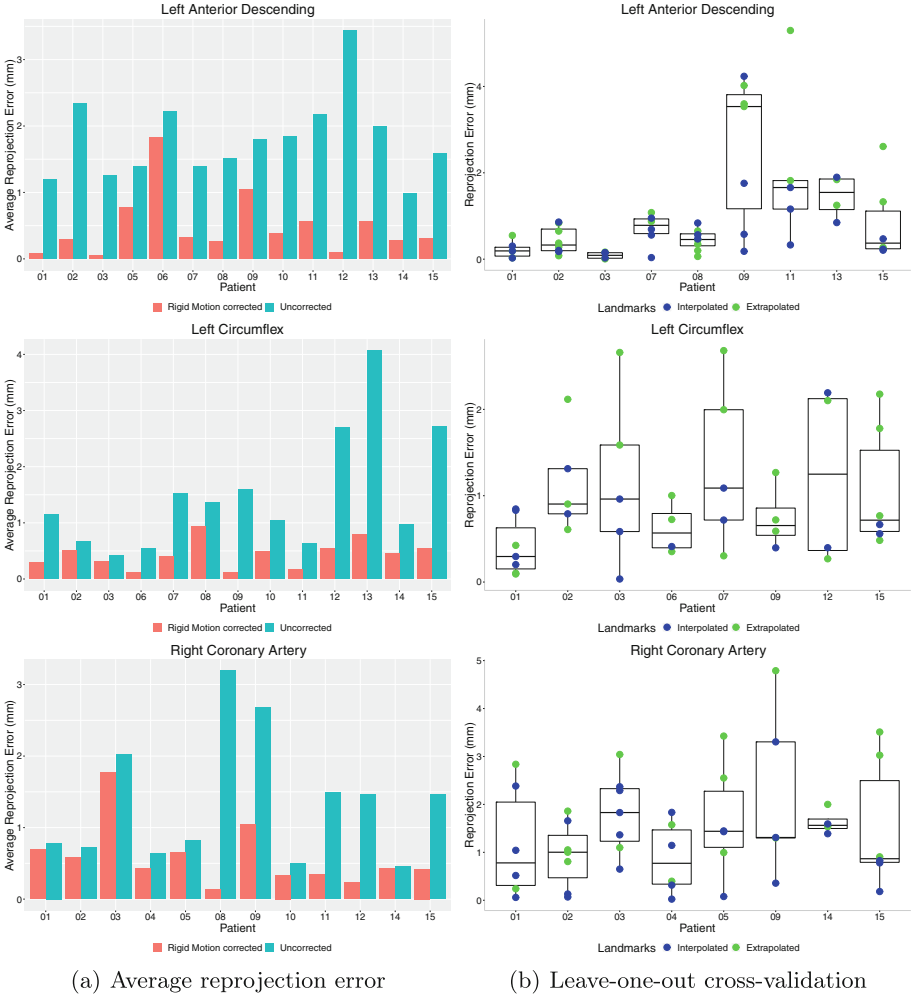
(a) Average reprojection error   (b) Leave-one-out cross-validation

Fig. 2. (a) Average reprojection errors of the landmarks after rigid motion correction; (b) Box plot of the reprojection errors of landmarks for leave-one-out cross-validation.

correction approach requires at least 4–6 bifurcation points, as landmarks, for its optimal performance and typically takes 10–25 iterations to converge.

The performance of the proposed technique is quantitatively measured by comparing the 2D landmarks with the back-projections of motion-corrected 3D landmarks on each of the projection plane. For initial quantitative evaluation, the average reprojection errors of the landmarks after rigid motion correction, along with the same without motion correction, are presented separately for LAD, LCx, and RCA as multiple-bar diagram in Fig. 2(a). The average reprojection errors of complete patient cohort after rigid motion correction are measured as 0.490 mm, 0.438 mm, and 0.591 mm for the LAD, LCx, and RCA, respectively.

The overall reprojection error combining all three arteries is measured as 0.504 mm. From every case presented in Fig. 2(a), it is clearly visible that the proposed approach significantly reduces the motion artifacts from all 2D projections of all coronary arteries.

For the final quantitative evaluation, we used the leave-one-out cross-validation technique. For each artery of every patient, one landmark point is selected and the rigid motion correction is performed based on the rest of the landmarks. Finally, on the rigid motion corrected projection planes, the reprojection error is estimated from the remaining landmark point. The procedure is applied on all landmark points for each of the LAD, LCx, and RCA and the results, in form of box plot, is presented in Fig. 2(b). Since the landmarks are situated either inside the arteries or at the end locations (proximal or distal), their locations are either interpolated or extrapolated after the rigid transformation. Hence, the reprojection errors corresponding to interpolated and extrapolated landmarks are represented using different colors in Fig. 2(b). Since our proposed algorithm requires at least 4 landmark points for its optimal performance, the leave-one-out cross-validation technique is only applicable when we have selected at least 5 landmarks. Hence, the number of cases have been reduced (9, 8, and 8 for LAD, LCx, and RCA, respectively) during our second analysis.

4   Discussion and Conclusions

Several 3D CA tree reconstruction methods have been developed in the past two decades. However, most of the existing methods either did not consider the effects of motion artifacts or followed the breath-hold and no patient movement protocol during image acquisition. In this regard, our objective is to propose a new retrospective rigid motion correction technique, keeping the standard clinical image acquisition protocol. The main advantage of the proposed approach is that it does not actually try to remove the effects of motion artifacts in projection domain, but re-orient the 3D x-ray C-arm system for optimal estimation of rigid transformation between angiogram acquisitions. The proposed algorithm tries identify how the same 2D angiographic projections can be generated if no motion artifact is involved, by optimally orienting the 3D vascular structure, along with the x-ray sources and projection planes.

In our experimental analysis, the average reprojection error for the RCA is higher than that of both LAD and LCx. The underlying reason is that, since the RCA passes along the atrioventricular groove, the effects of residual non-rigid motion artifacts (heart stretching and shrinking due to cardiac motion) in RCA is comparatively higher than in LCA. The height of box plots, presented in Fig. 2(b), is often quite high (high interquartile range) in our data. The reason behind is that the box plots are computed over reprojection errors of both interpolated and extrapolated landmarks and hence, has high degree of variation. Also, since the number of landmarks at each artery are very limited (5–8), the extrapolated landmarks, which tend to have comparatively higher reprojection errors, are considered inside the data distribution, instead of being treated as an

outlier. Despite that, the box plots corresponding to LAD have less dispersion (except one), demonstrating the effectiveness of proposed approach.

The objective of the proposed rigid motion correction algorithm is to enable accurate identification of point correspondences between vessels, or vessel centerlines, from multiple x-ray angiograms. This will allow the development of a completely automated 3D CA tree reconstruction method that, when embedded in an x-ray angiogram system, will generate the 3D rendering of coronary vascular structure during cardiac intervention, as well as automatically estimate physiological information, such as severity of the coronary stenoses.

References

1. Banerjee, A., Kharbanda, R.K., Choudhury, R.P., Grau, V.: Automated motion correction and 3D vessel centerlines reconstruction from non-simultaneous angiographic projections. In: Pop, M., et al. (eds.) STACOM 2018. LNCS, vol. 11395, pp. 12–20. Springer, Cham (2019). https://doi.org/10.1007/978-3-030-12029-0_2
2. Cañero, C., Vilariño, F., Mauri, J., Radeva, P.: Predictive (un)distortion model and 3-D reconstruction by biplane snakes. IEEE Trans. Med. Imaging **21**(9), 1188–1201 (2002)
3. Çimen, S., Gooya, A., Grass, M., Frangi, A.F.: Reconstruction of coronary arteries from X-ray angiography: a review. Med. Image Anal. **32**, 46–68 (2016)
4. Chen, S.J., Schäfer, D.: Three-dimensional coronary visualization, part 1: modeling. Cardiol. Clin. **27**(3), 433–452 (2009)
5. Cong, W., Yang, J., Ai, D., Chen, Y., Liu, Y., Wang, Y.: Quantitative analysis of deformable model-based 3-D reconstruction of coronary artery from multiple angiograms. IEEE Trans. Biomed. Eng. **62**(8), 2079–2090 (2015)
6. Eng, M.H., et al.: Impact of three dimensional in-room imaging (3DCA) in the facilitation of percutaneous coronary interventions. J. Cardiol. Vasc. Med. **1**, 1–5 (2013)
7. Galassi, F., Alkhalil, M., Lee, R., Martindale, P., et al.: 3D reconstruction of coronary arteries from 2D angiographic projections using non-uniform rational basis splines (NURBS) for accurate modelling of coronary stenoses. Plos One **13**(1), 1–23 (2018)
8. Holland, A., Goldfarb, J., Edelman, R.: Diaphragmatic and cardiac motion during suspended breathing: preliminary experience and implications for breath-hold MR imaging. Radiology **209**(2), 483–489 (1998)
9. Horn, B.K.P.: Closed-form solution of absolute orientation using unit quaternions. J. Opt. Soc. Am. A **4**(4), 629–642 (1987)
10. Husmann, L., Leschka, S., Desbiolles, L., Schepis, T., et al.: Coronary artery motion and cardiac phases: dependency on heart rate - implications for CT image reconstruction. Radiology **245**(2), 567–576 (2007)
11. Mark, D.B., et al.: ACCF/ACR/AHA/NASCI/SAIP/SCAI/SCCT 2010 expert consensus document on coronary computed tomographic angiography: a report of the american college of cardiology foundation task force on expert consensus documents. J. Am. Coll. Cardiol. **55**(23), 2663–2699 (2010)

12. Shechter, G., Resar, J.R., McVeigh, E.R.: Displacement and velocity of the coronary arteries: cardiac and respiratory motion. IEEE Trans. Med. Imaging **25**(3), 369–375 (2006)
13. Wiesent, K., Barth, K., Navab, N., Durlak, P., et al.: Enhanced 3-D-reconstruction algorithm for C-arm systems suitable for interventional procedures. IEEE Trans. Med. Imaging **19**(5), 391–403 (2000)